Supplements

Table S 1: Lists of EANET stations grouped by their countries with ID number as in Error! Reference source not found.**.**

Country	Station (ID number)
Cambodia	PhnomPenh (31)
China	Jinyunshan (48), Hongwen (14)
Indonesia	Jakarta (18), Serpong (36), Bandung (1)
Japan	Rishiri (33), Ochiishi (26), Tappi (38), Sado-seki (34), Happo (10), Ijira (15), Oki (28), Banryu (3), Yusuhara (45), Hedo (11), Ogasawara (27), Tokyo (40)
Lao	Vientiane (42)
Malaysia	Petaling Jaya (30), Tanah Rata (37), Danum Valley (7)
Mongolia	Ulaanbaatar (41), Terelj (39)
Myanmar	Yangon (43), Mandalay (50)
Philippines	Metro Manila (22), Mt. Sto. Tomas (24)
Republic of Korea	Kanghwa (19), Cheju (Kosan) (5), Imsil (16)
Russia	Mondy (23), Listvyanka (21), Irkutsk (17), Primorskaya (32)
Thailand	Bangkok (2), Samutprakarn (47), Pathumthani (29), Khanchanaburi (20), Chiang Mai (6), Sakaerat (35), Nai Mueang (25), Chang Phueak (46), Si Phum (49)
Vietnam	Hanoi (8), Hanoi (Relocated) (9), Hoa Binh (13), Can Tho (4), Ho Chi Minh (12), Yen Bai (44)

Table S 2: Model comparison with ATom1 flights, calculated for all flight, and for North Pacific (NP) region: no outlier detection is applied. N is number of available data for each calculation, R is the correlation coefficients. *R* and bias of the STD run are shown as bold if better than that of the OLD run. Unit of bias is ppt for NO_2, OH, ppb for O_3, CO.

	NO_2	**NO_2 (NP)**	**O_3**	**O_3 (NP)**	**OH**	**OH (NP)**	**CO**	**CO (NP)**
N	29,509	2,283	29,204	2,246	7,601	608	27,467	2,172
R (STD)	**0.730**	**0.621**	0.751	**0.609**	0.579	**0.407**	**0.659**	**0.596**
R (OLD)	0.697	0.306	0.752	0.598	0.584	0.374	0.643	0.596
bias (STD)	-11.277	**0.588**	**11.637**	**8.471**	-0.038	**-0.003**	**1.698**	**-1.713**
bias (OLD)	-6.940	4.450	15.025	13.050	-0.015	0.015	-7.521	-12.393

Table S 3: Additional sensitivity runs for the EMeRGe comparison.

The AIRC case aims to evaluate source of HONO from aircraft emissions of HONO using a HONO/NO_x emission factor of 0.4. In the EMx8 case, the HONO/NO_x emission factor is amplified up to 0.8 (=0.1 in STD case) to emphasize the sensitivity of HONO's direct source from the ground layer, especially from soils (Oswald et al., 2013). In the GRx8 case, the rate constant of (R2) is eightfold to increase homogeneous HONO production, given that daytime missing HONO could relate to other gas-phase formations (Romer et al., 2018; Li et al., 2014). The factor 8 applied in EMx8 and GRx8 cases are selected after testing with factors 2 and 4, aiming for simulations to agree with the measurements.

No.	Simulation ID	Description	Note
1	AIRC	aircraft HONO emission = 0.4% aircraft NO_x emission	Not applied in STD
2	GRx8	Rate (R2) × 8	
3	EMx8	EM(HONO) = 0.8 NO_x emission	= 0.1 in STD

Table S 4: Tables of correlation coefficient (*R*) and model biases against EMeRGe measurements for HONO.

"Alt." columns show altitude ranges (±500 m). "*N*" column show the numbers of hourly-averaged values calculated for each altitude range. Left table: darker colours represent higher absolute values of *R* (closer to ±1). Right table: lighter colours show smaller model biases (closer to 0). The darkness of blues (negative values) and reds (possitive values) are scaled to ±1 for *R* and ±maximum values of each row for biases. Unit of biases is ppt for HONO and NO_2, ppb for O_3 and CO.

		***R*(HONO)**										
Alt.	***N***	**STD**	**GRx8**	**EMx8**	**AIRC**	**maxST**	**ratR4**	**ratR4 +CLD**	**JANO3-B**	**JANO3-C**	**maxST+ JANO3-B**	**maxST+ JANO3-C**
0	970	-0.23	-0.39	-0.29	-0.27	-0.17	-0.22	-0.21	0.63	0.62	0.64	0.63
1000	1714	0.49	0.36	0.51	0.44	0.56	0.24	0.24	0.36	0.37	0.48	0.48
2000	1538	0.31	0.47	0.38	0.36	0.47	0.12	0.07	0.47	0.40	0.41	0.39
3000	2296	0.16	0.05	0.11	0.11	-0.03	0.13	0.05	0.34	0.28	0.18	0.26
4000	192	-0.17	-0.24	-0.08	-0.11	0.28	-0.11	-0.04	0.08	-0.14	0.36	0.30
5000	836	0.04	0.03	0.14	0.21	0.53	0.19	0.75	0.17	-0.22	0.49	0.06
6000	506	-0.01	0.02	-0.03	0.03	0.11	-0.03	0.05	0.10	-0.26	0.16	-0.12
7000	76	-0.31	-0.33	-0.31	-0.33	-0.30	-0.30	-0.30	-0.29	-0.29	-0.27	-0.22
8000	44	-0.67	-0.64	-0.64	-0.64	-0.64	-0.68	-0.67	-0.62	-0.65	-0.63	-0.59

		Bias(HONO)										
Alt.	***N***	**NEW**	**GRx8**	**EMx8**	**AIRC**	**maxST**	**ratR4**	**ratR4 +CLD**	**JANO3-B**	**JANO3-C**	**maxST+ JANO3-B**	**maxST+ JANO3-C**
0	970	-112.5	-94.1	-102.7	-112.2	-70.3	-106.1	-102.9	-21.7	-17.6	155.0	154.9
1000	1714	-105.3	-95.5	-94.2	-105.6	-71.7	-99.8	-96.1	-47.8	-40.8	65.9	72.3
2000	1538	-64.1	-62.9	-64.1	-64.4	-61.8	-63.3	-62.8	-53.1	-45.6	-32.5	-23.6
3000	2296	-44.2	-42.8	-44.1	-44.2	-43.2	-43.9	-43.7	-38.7	-30.2	-27.7	-16.2
4000	192	-26.0	-24.3	-25.8	-26.0	-25.6	-25.7	-25.4	-23.8	-17.9	-21.2	-14.4
5000	836	-18.9	-17.3	-18.8	-19.0	-18.5	-18.8	-18.3	-17.7	-12.8	-15.6	-9.6
6000	506	-5.0	-2.9	-4.6	-5.1	-4.9	-4.8	-4.8	-4.1	2.5	-3.9	2.2
7000	76	-4.1	0.7	-3.5	-4.3	-4.1	-3.8	-3.7	-2.3	1.5	-2.0	1.7
8000	44	-2.8	2.9	-1.9	-2.7	-2.7	-2.5	-2.5	-1.5	2.9	-1.2	3.5

Table S 5: **CH_4 lifetime and tropospheric abundances for NO_x, O_3, CO, and HONO and their changes by HONO chemistry in sensitivity cases.**

Simulation ID	CH_4 lifetime	Abundances of tropospheric			
	(yr)	NO_x (TgN)	O_3 (TgO_3)	CO (TgCO)	HONO (TgN)
OLD	9.09	0.119	408.79	327.20	
STD	10.28	0.094	388.21	354.57	1.40
maxST	14.54	0.048	323.80	425.31	7.79
ratR4+CLD	9.60	0.108	390.34	337.68	3.18
JANO3-A	10.05	0.096	391.11	349.91	1.45
JANO3-B	7.60	0.116	426.89	292.29	2.02
JANO3-C	5.39	0.153	477.48	237.59	2.93
maxST+JANO3-B	10.20	0.057	351.27	357.27	12.64
maxST+JANO3-C	6.44	0.084	408.69	268.74	17.13
Effects		Changes (%) vs OLD			vs STD
By STD	+13.05	-20.40	-5.03	+8.36	
by maxST	+50.65	-55.44	-17.84	+37.02	+634.51
by ratR4+CLD	+5.60	-8.57	-4.51	+3.20	+129.94
By JANO3-A	+10.57	-18.97	-4.32	+6.94	+3.42
By JANO3-B	-16.39	-2.49	+4.43	-11.06	+44.2
By JANO3-C	-40.74	+28.89	+16.08	-32.41	+108.7
By maxST+JANO3-B	+12.21	-52.10	-14.07	+9.19	+802.86
By maxST+JANO3-C	-29.15	-29.41	-0.02	-17.87	+1123.57

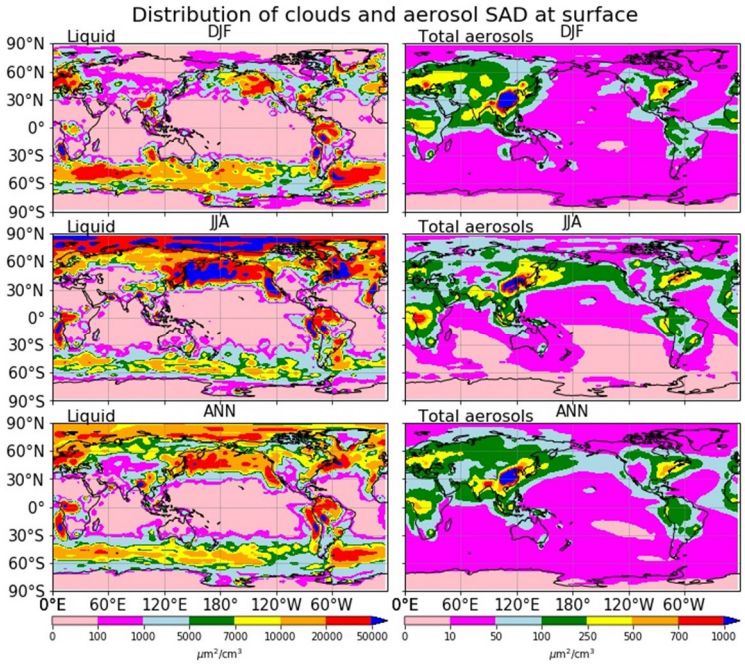

35

Figure S 1: Seasonal and annual mean distributions of cloud droplet (left) and total aerosols SAD (right).

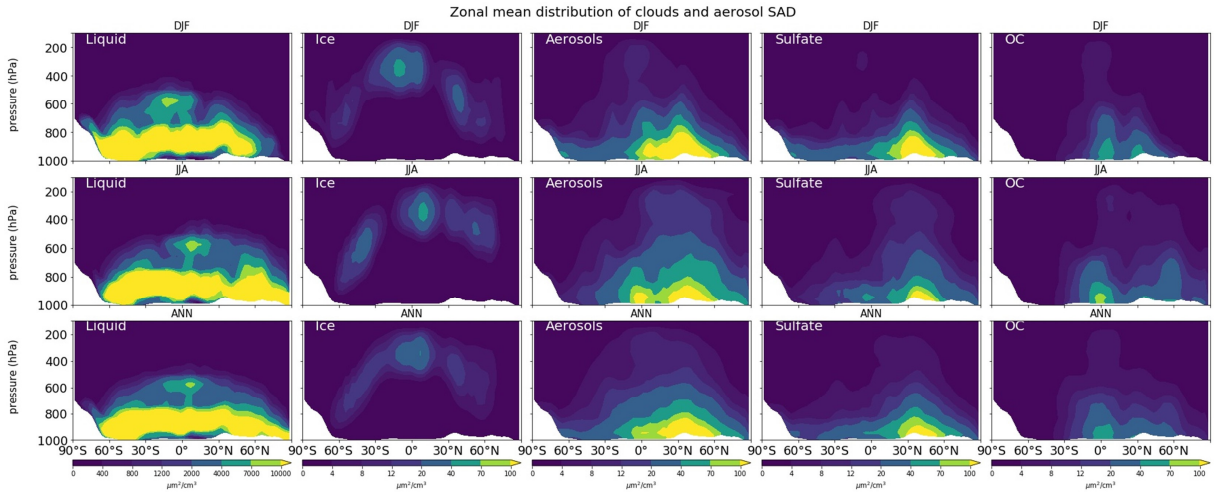

Figure S 2: Zonal, seasonal mean (upper and middle panels), and annual mean (lower panels) distribution of cloud droplet surface aerosol density (SAD), cloud ice SAD, total aerosol SAD, sulfate aerosol SAD, and organic carbon SAD (from left to right).

40

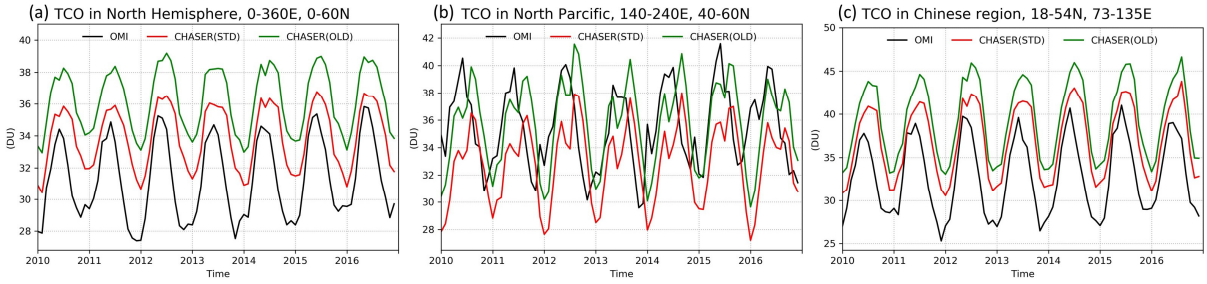

Figure S 3: Verifications with OMI satellite data for tropospheric column ozone (TCO). TCO (DU) by OMI (black) and CHASER (red: STD case; green: OLD case) in the Northern Hemisphere (a), NP (b), and Chinese (c) regions are plotted.

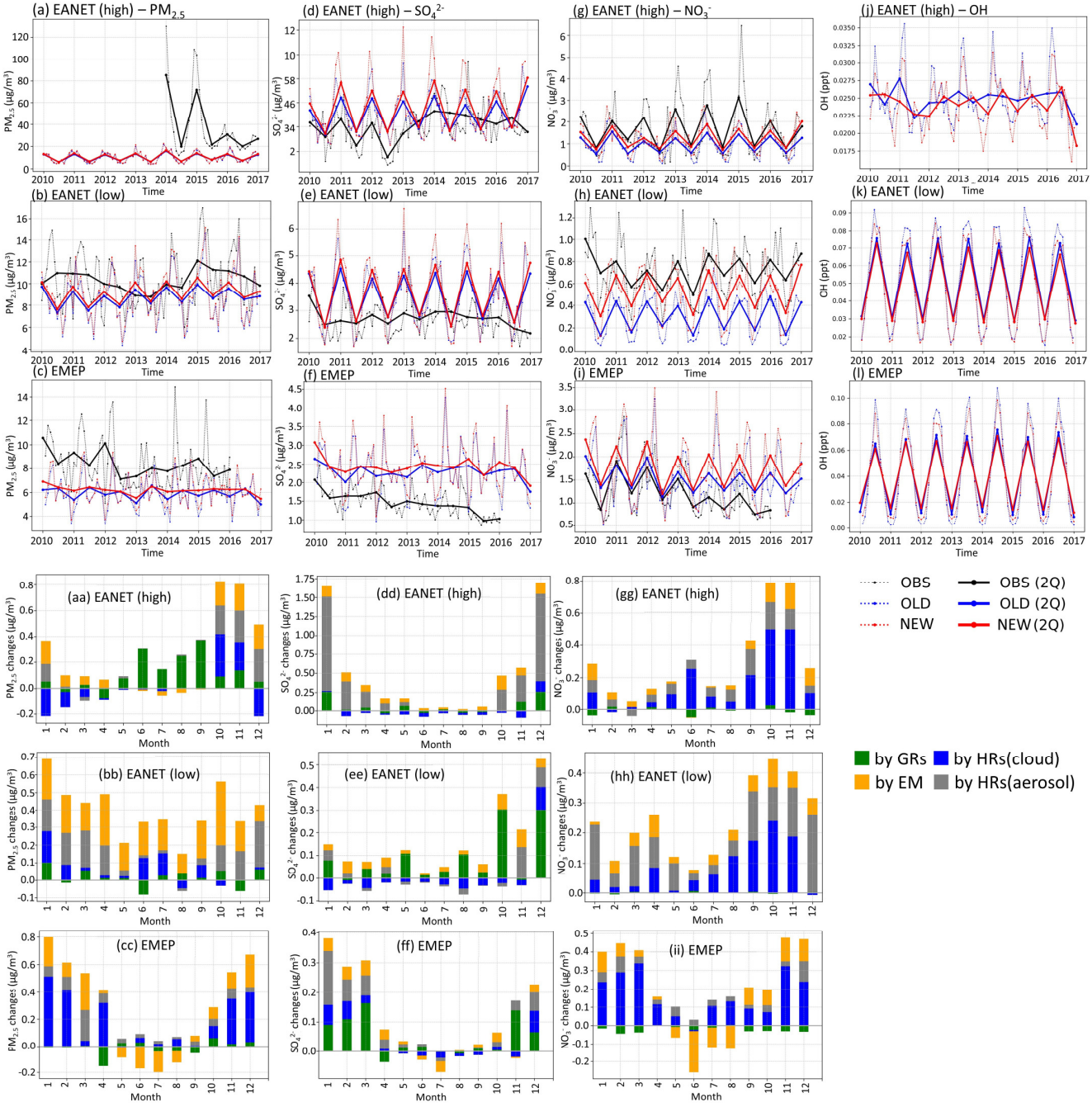

Figure S 4: Observed and simulated mass concentrations (a-l) and monthly-mean changes (aa-ii) for $PM_{2.5}$, SO_4^{2-}, and NO_3^-, and OH for EANET and EMEP stations, grouped as high-NO_x EANET, low-NO_x EANET, and all EMEP stations. In (a-m), black lines: observation; red: STD case; blue: OLD case. Dotted lines are all stations' median from monthly-mean for each station in that group. Thick solid lines represent two quarters averaged from dotted lines. Noted that for OH's plots (j-l), there are no observational data and only values from STD and OLD simulations are presented. In (aa-ii), green bars: monthly changes by GRs; blue: by HRs on clouds; grey: by HRs on aerosols; orange: by EM.

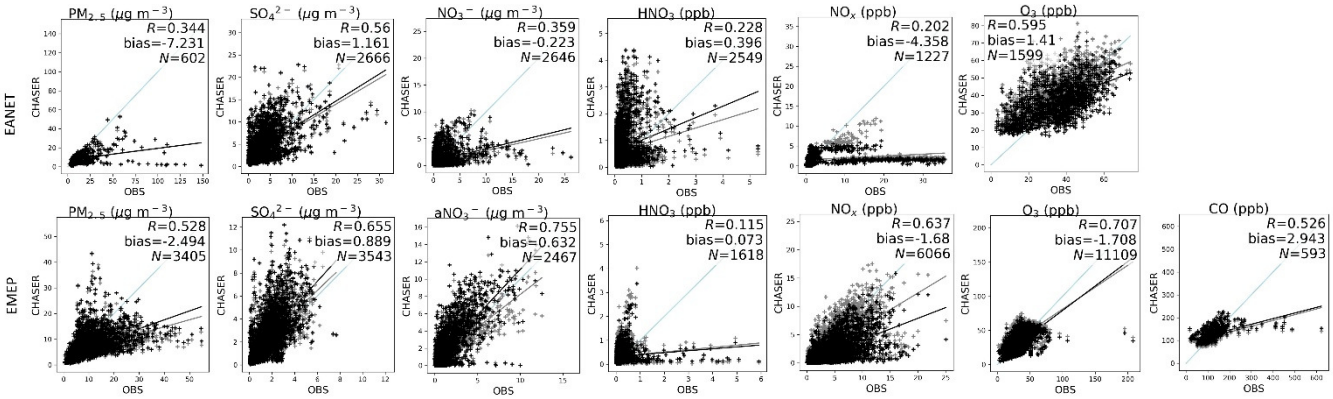

Figure S 5: Correlations of STD and OLD runs with EANET (upper) and EMEP (lower) stations for $PM_{2.5}$, SO_4^{2-}, NO_3^-, HNO_3, NO_x, O_3, and CO (CO for EMEP only). Fitting lines for STD (black) and OLD (grey) with observations are also plotted. *N* (no unit) is the number of available data after outlier filtering, which is similar as described in Error! Reference source not found.**.**

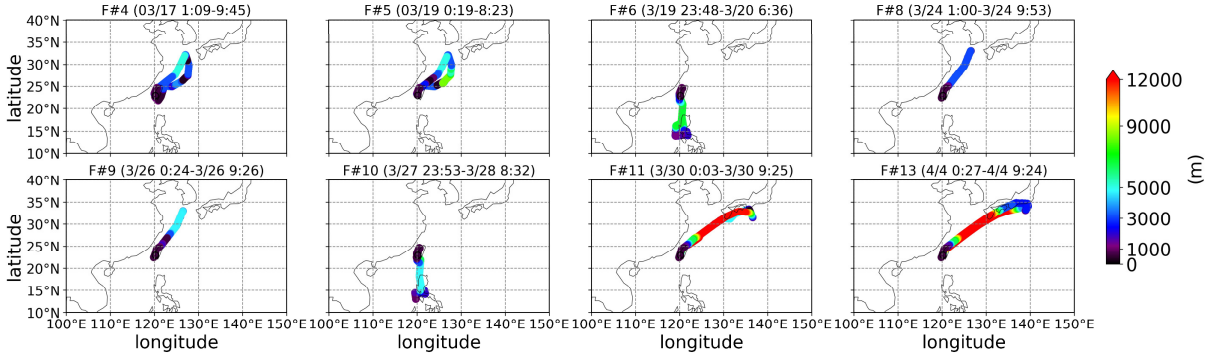

Figure S 6: Cruishing altitudes in EMeRGe-Asia 2018 campaign.

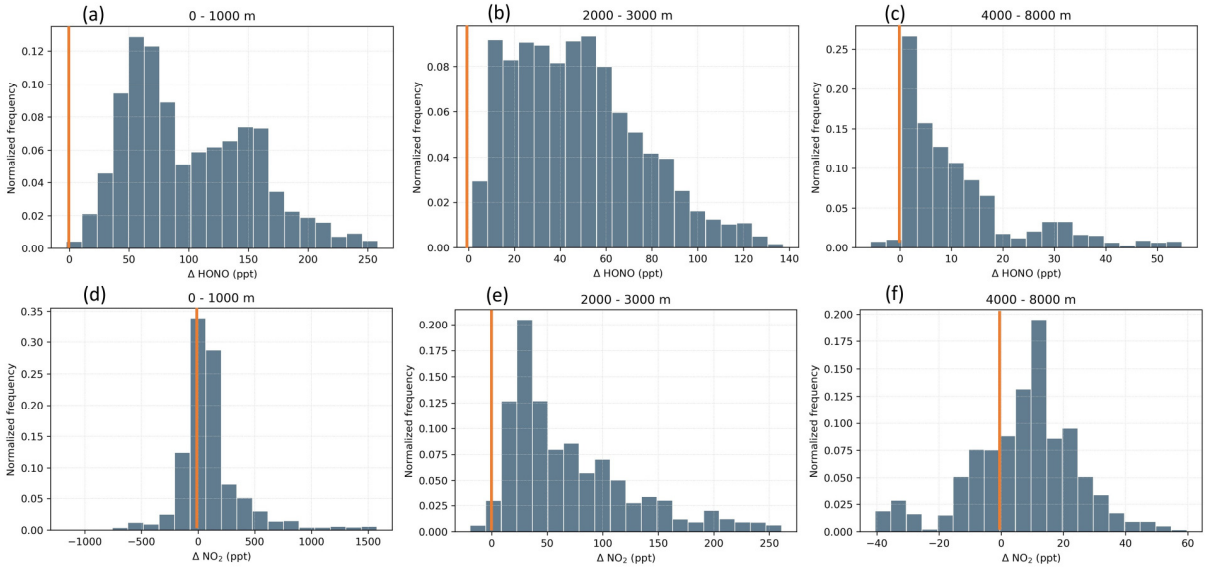

Figure S 7: Normalized distributions of the differences between measured and simulated data (OBS – STD) for HONO (upper panel) and NO_2 (lower panel). Data are separated into three categories (±500 m): 0 – 1000 m (a-d), 2000 – 3000 m (b-e), 4000 – 8000 m (c-f). Three-sigma-rule outlier detection is applied for each altitude range before grouped.

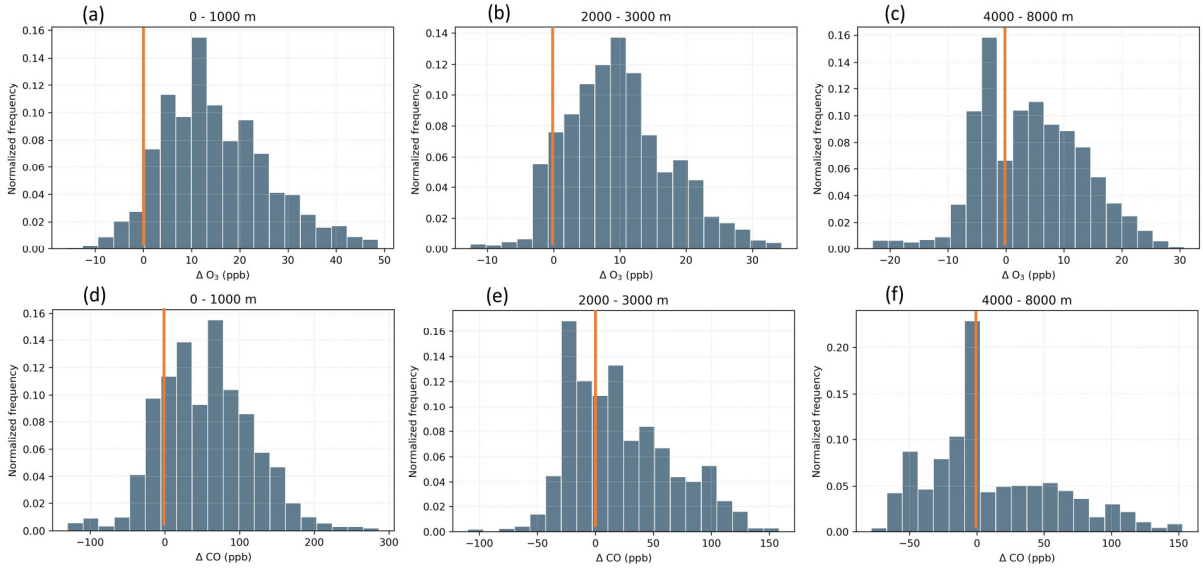

Figure S 8: Normalized distributions of the differences between measured and simulated data (OBS – STD) for O_3 (upper panels) and CO (lower panels). Data are separated into three categories (±500 m): 0 – 1000 m (a-d), 2000 – 3000 m (b-e), 4000 – 8000 m (c-f). Outliers of each altitude group are filtered by 3-order rule.

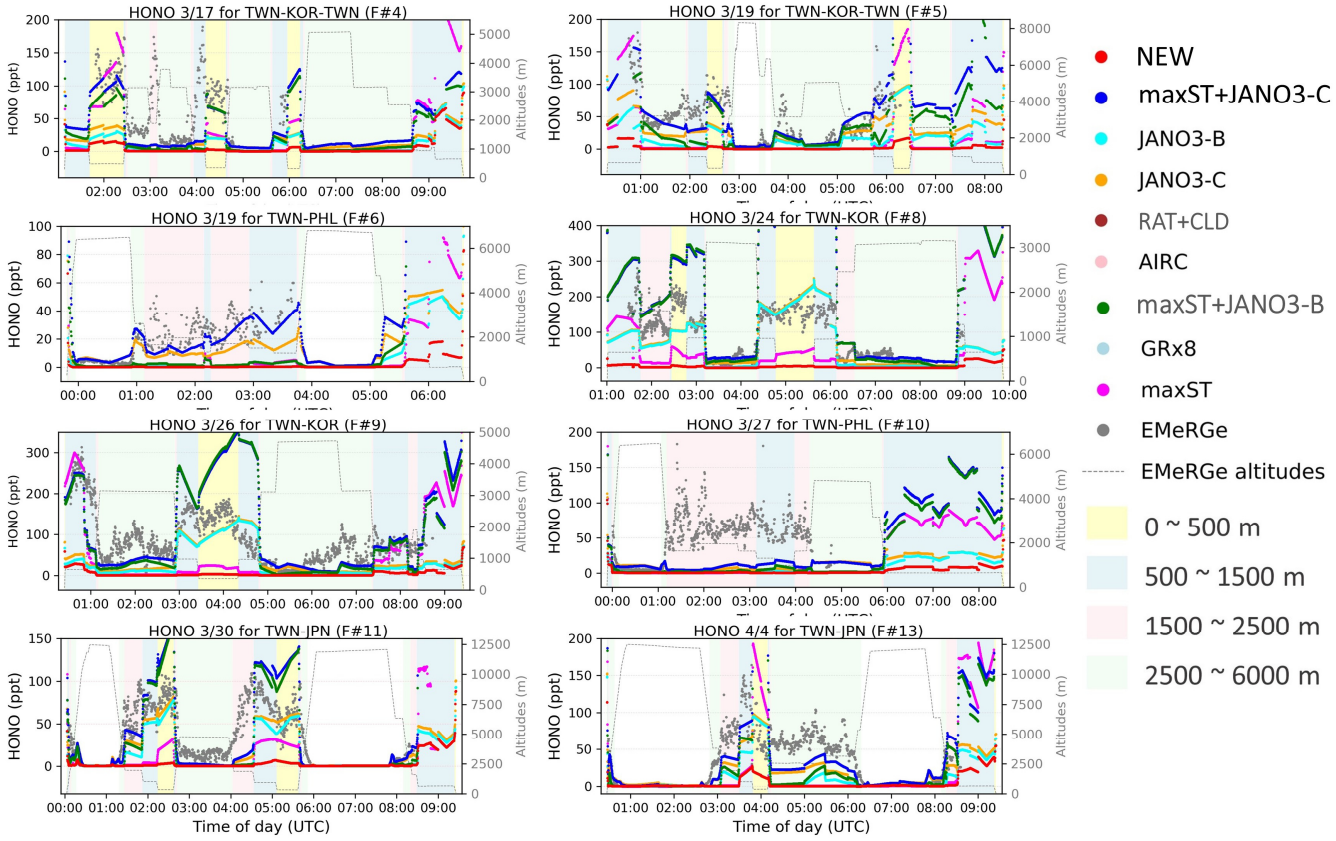

Figure S 9: HONO concentrations measured in EMeRGe flights. The observational values (grey dots), the NEW case (red), the maxST case (magenta), maxST+JANO3-B case (green lines), and maxST+JANO3-C cases (blue lines) are plotted. Flight altitudes (metres) are plotted in light dash lines scaled to the right axis. Vertical background columns indicate altitude ranges.

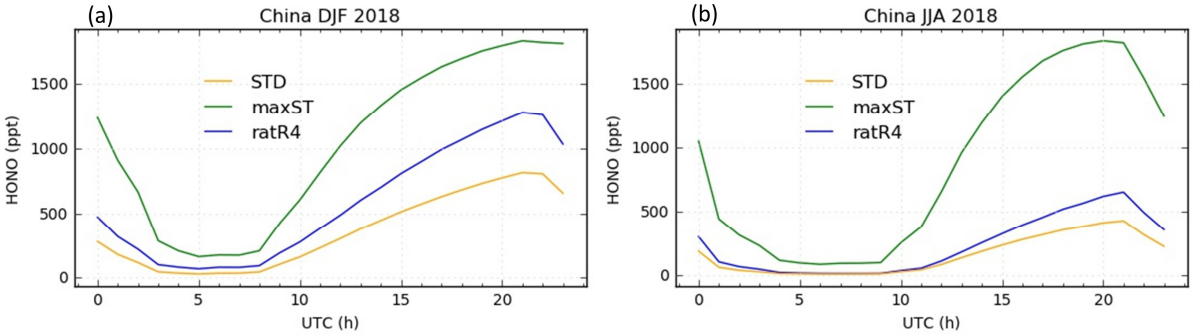

Figure S 10: Diurnal variance of HONO at the surface of Chinese region in December, January, February (a), and June, July, August (b). Orange lines show STD run; green lines show maxST run; blue lines show ratR4 run. In (b), the averaged summer mean of HONO in surface air reached the maximum at 0.8 ppb in the STD simulation (orange), which substantially increased up to 1.8 ppb in maxST (green), which is closer to 2.0 ppb, as reported by Li et al. (2012).

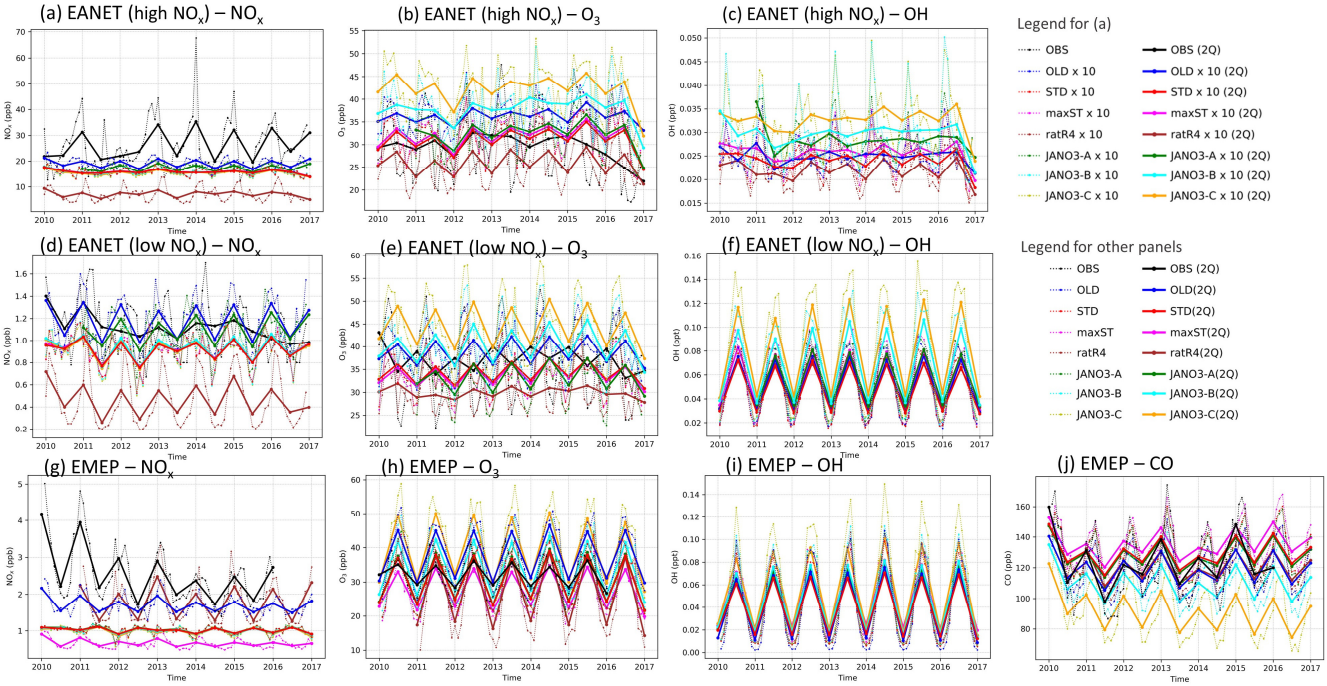

Figure S 11: Concentrations of NO_x, O_3, OH, and CO for EANET and EMEP stations by observation and various simulations. The upper legend block indicates simulated NO_x concentration is tenfolded for high-NO_x EANET stations (a panel). The lower legend block is for the other panels of the figure.

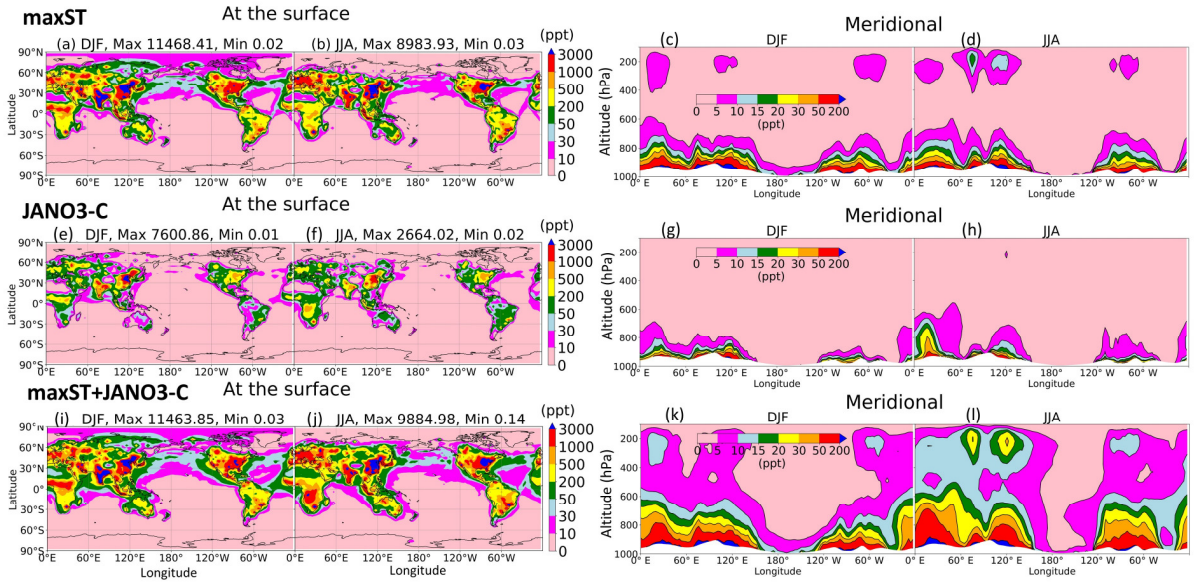

Figure S 12: HONO production in maxST (a-d), JANO3-C (e-h), and maxST+JANO3-C cases (i-l) at the surface layer (left panels) and meridional (right panels).

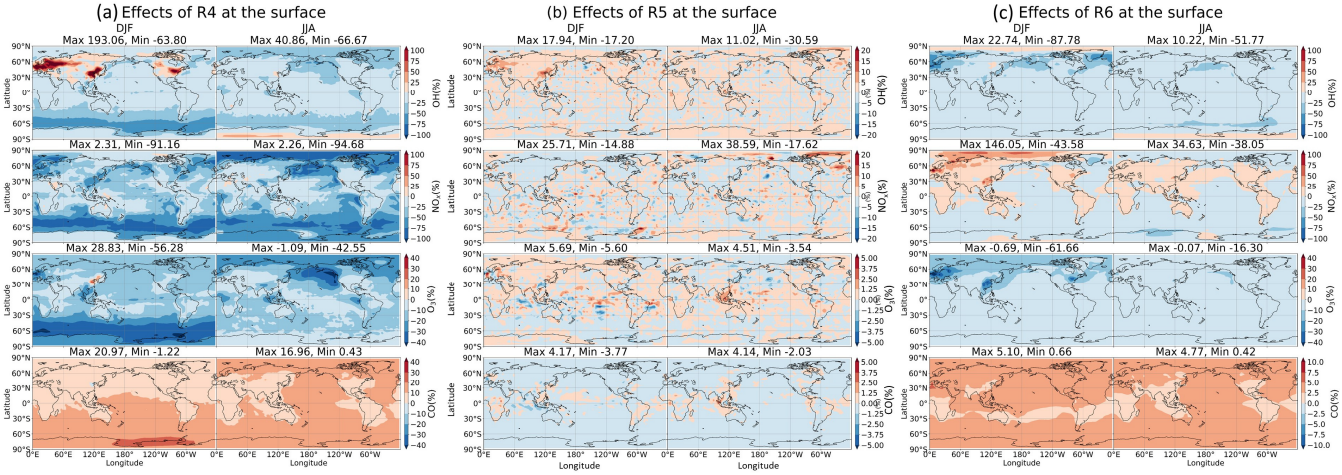

Figure S 13: **Changes in the surface OH, NO_x, O_3, and CO concentrations by (R4), (R5), and (R6). The colorbar scale for each panel are different; (a) OH, NO_x (-100,100), O_3, CO (-40,40), (b) OH, NO_x (-20,20), O_3, CO (-5,5), (c) OH, NO_x (-100,100), O_3 (-40,40), CO (-10,10). Unit is %.**

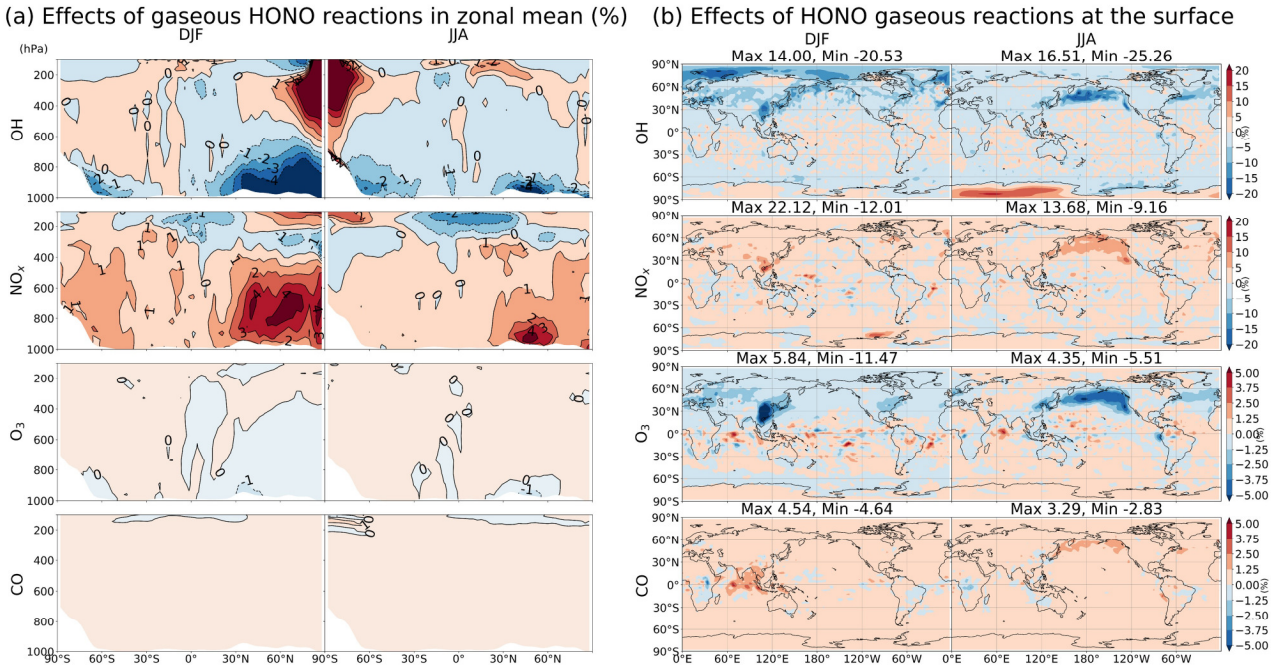

Figure S 14: **Changes (%) in zonal mean (a) and at the surface (b) for OH, NO_x, O_3, and CO concentrations by gaseous HONO chemistry (R1, R2, R3). The colorbar scale for each panel are different.**